

APPLICATIONS OF X-RAY COMPUTED TOMOGRAPHY TO COAL STUDIES

D.H. Maylotte, P.G. Kosky, E.J. Lamby, C.L. Spiro

General Electric Corporate Research and Development
Schenectady, NY 12301

and

A. Davis, D.F. Bensley

Pennsylvania State University
University Park, PA 16802

X-ray computed tomography (CT) is a non-destructive, non-invasive technique which has been applied here to studies of the internal structures of coal and the penetration of tracer gas into those structures. The CT images are 2-D cross-sectional images of the coal rather than the shadowgraphs of traditional radiography. Compared to shadowgraphs, the CT images provide higher spatial and higher density resolution.

CT images are digital images of the effective x-ray attenuation coefficient for elementary volumes (voxels) within the sample. In these experiments a GE 8800 CT/T machine was used to take the image data, which were then reconstructed to product images with a voxel size of 0.3 mm x 0.3 mm x 1.5 mm. The CT number for each voxel is related to the experimental effective attenuation coefficient for that volume by the relationship:

$$\text{CT No.} = 1024 \times \left[1 + \frac{\mu(\text{material})_E - \mu(\text{water})_E}{\mu(\text{water})_{E_0}} \right]$$

where $\mu(\text{material})_E$ is the attenuation coefficient for the unknown material, $\mu(\text{water})_E$ is the attenuation coefficient of water taken under the same conditions, and $\mu(\text{water})_{E_0}$ is the attenuation coefficient of water taken under standard conditions. The CT images were displayed by assigning a grey scale to the CT numbers. The whiter the image the higher the CT number represented by it and the higher the electric density of the sectioned object. The data collection time for each image was nine seconds.

The x-ray tube for this work was operated at 120 Kev. The filtered emission is a continuum covering the range 20 Kev - 120 Kev, peaking at 35 Kev (Ref. 1). Over this energy range the three significant attenuation mechanisms are, (i) photoelectric absorption, (ii) Compton scattering, and (iii) coherent scattering. For carbonaceous materials the dominant mechanism in this energy range is Compton scattering; therefore, the CT images reflect the electron density distribution within the sample. For the low atomic number elements commonly found in coal the atomic weight is almost twice the atomic number (hydrogen contributes little to the total electron density) and therefore the images are approximately images of the mass density within the sample.

Figure 1 shows a CT image of a piece of Illinois #6 coal. The piece was cut from a larger block which, after mining, had been stored in a sealed vessel under deionized water. The dimensions of the piece were 2.5 cm x 2.5 cm x 10 cm long. The long axis was cut parallel to the bedding planes of the coal. This CT image was taken perpendicular to the

long axis of the coal piece. The coal was potted in a cylinder of epoxy which was then cut to expose the two smaller end faces of the coal and finally O-ring sealed in an acrylic plastic tube (5 cm I.D.).

A sample rectangle on the coal image has been displayed in Figure 1a, and a histogram of the CT values within that rectangle is shown in Figure 1b. Both the average and most probable CT number in the area was 1220. Subsequent to the CT experiments, this particular piece of coal has been sectioned along the plane whose structure was examined by the x-ray fan beam. A microlithotype examination of the exposed face showed that the predominant material in the region covered by the sample rectangle is vitrain. A number of bituminous coals have been examined by CT and, after sectioning, petrographically. CT numbers in the range 1210-1250 are the most commonly occurring numbers in these coals. This assignment of a CT number of circa 1210 to vitrain is also justified on theoretical grounds.

The CT number for a particular material can be calculated when the following system characteristics are known, (a) the emission spectra for the filtered source, (b) the elemental composition and number density of the material being examined, (c) the wavelength sensitivity and efficiency of the detection system. The results of such a calculation for a number of standard materials, minerals and for coal are given in Table 1.

Material	CT (Calc.)	CT (Obs.)
Coal (C ₄₉ H ₄₃ O ₇ S ₁ N ₁)	1254	~ 1220
Kaolin (Al ₄ Si ₄ O ₁₀ (OH) ₈)	3096	3078
Teflon C ₂ F ₄	2106	2050
Calcite CaCO ₃	4521	> 4096
Dolomite CaMg(CO ₃) ₂	3924	3900-4096
Water H ₂ O (standard)	1024	

TABLE 1: Calculated and Actual CT Numbers for Coal and Minerals

The calculation of the theoretical CT value for coal assumed the formula given in Table 1 and a density of 1.3 g.cm⁻³. The calculated CT number is not significantly affected by the formula chosen to represent coal within the reasonable limits of the formulas for the three major maceral groups, i.e., vitrinite, exinite, and inertinite (2). However, the CT number is directly affected by the density chosen for the coal. This insensitivity of CT number to the formula of a hydrocarbonaceous material and its sensitivity to the density is demonstrated in Figure 2. In the density range around 1.3 g/cc the density sensitivity of the technique is 11 CT numbers for a 1% density change. For a uniform material the standard deviation of the CT numbers is ± 2. The different maceral groups in coal have different densities in the range 1.1 to 1.6 g/cm³ (2), and the CT image has enough density resolution to distinguish between them. However, the normal size range of many individual coal macerals is below the spatial resolution of the CT equipment being used in this work. In the present experiments, a CT voxel represents a volumetric average of the densities of the macerals contained within it.

In the case of kaolin the CT number for the bulk sample reflects the porosity of the kaolin as well as the CT number attributable to the mineral itself. The kaolin sample was therefore potted in a low viscosity epoxy resin which penetrated the outer layers of the sample (Figure 3). The CT number for the kaolin mineral and the void fraction within the kaolin can then be calculated from the relationships:

$$CT_{total}(1) = \epsilon \times CT_{epoxy} + (1-\epsilon) CT_{kaolin} \quad 1)$$

$$CT_{total}(2) = \epsilon \times (CT \# \text{ of air} = 0) + (1-\epsilon) CT_{kaolin} \quad 2)$$

where ϵ is the void fraction in the mineral. The Equation 1) was evaluated for a region where epoxy had penetrated the kaolin and Equation 2) was evaluated for a region inside the kaolin where the epoxy has not penetrated and air fills the spaces between the kaolin grains. The CT number for the cured epoxy was taken from the region outside of the mineral. The CT number for kaolin as obtained in this calculation is given in Table 1 and the void fraction in the bulk mineral was found to be 38%.

The results of Table 1 show that if a region of coal has a CT number above 1300 but less than 3100 then it is contaminated with a varying proportion of mineral matter, and if the CT number is greater than 3100 then it is contaminated with high atomic number minerals (e.g., calcite or pyrite). If the CT number is between 1100 and 1400 then the area is essentially organic, while if it is below 1000 then the area contains an unusually large component of voids.

The CT number for a particular volume of the imaging space is affected by the amount and density of the coal present, the minerals present, and the void space in that volume. Because of the large CT numbers associated with the mineral matter (Table 2), the mineral content of the CT volume would be expected to have a large effect upon the CT image.

Figure 4 shows the same CT image as in Figure 1a, but this time a reference line has been drawn over the image and the CT numbers plotted along that line. The white area at the bottom left of the image corresponds to the peak in CT number on the left-hand side of the graph.

After the CT experiments had been completed, and the coal sectioned along the CT image plane, automated x-ray microprobe measurements were made along the same region as the line in the CT image. The area of the microprobe beam was $50 \mu\text{m} \times 50 \mu\text{m}$ with an expected penetration of ca $1 \mu\text{m}$. The elements scanned in the microprobe were Si, Al, S, Fe, Mg, Na, K, Ca. The observed weight percents for the elements were totalled and plotted against distance (Figure 5). The automated microprobe measurements are in a finer grid than the CT data. If converted to the same grid size as the CT, then peaks in the microprobe spectra would appear shorter and broader. There does appear to be a first order correlation between the mineral matter in the coal and the variation in density of the CT image. CT images of raw coal can be regarded therefore as maps of the mineral distribution within the coal. A further distinction into minerals of elements with high atomic number (e.g., pyrite) and minerals with only low atomic number minerals (e.g., illite) may also be possible using images taken with different x-ray energies.

The porosity within this particular coal sample was examined by following the penetration of xenon gas into the sample at room temperature (27°C). Xenon was chosen because of its relatively inert nature and because it has a strong x-ray K-absorption edge at 35 Kev, i.e., at the peak of the spectrum from the x-ray tube. The presence of xenon should therefore be detectable against the coal background. The penetration of xenon gas

into the coal was carried out by exposing one end face of the coal parallelepiped to a pressure of xenon (1130 torr) and monitoring the gas exiting the opposite face by following the pressure rise in a closed system of known volume. The penetration of gas within the coal was monitored, (a) with the coal containing its equilibrium moisture, (b) after the coal had been dried at 80°C for two weeks. The bulk gas flow through the coal was much faster in case (b) than in (a). After about 3.5 hours the pressure on both sides of the coal had equalized in case (b). Images from the second series of experiments are more indicative of the porosity within the coal and three images from these experiments are shown in Figure 6. These images were obtained by subtracting the digital image of the evacuated coal from the digital images taken while the xenon was penetrating into the coal. The resulting difference image is a map of xenon penetration. The images clearly show the non-uniform nature of the penetration of the xenon into the coal. The lighter areas in the image are the areas into which the xenon has preferentially penetrated. The plane of the CT image was situated about 15 mm in the coal block from the high pressure end. The presence of xenon in this plane was detected in the first image taken of this plane after the xenon had been introduced into the high pressure chamber (time elapsed was eight minutes). The major features of the pattern were streaks of xenon parallel to the bedding planes of the coal. Over the duration of the experiment these features grew in intensity and broadened out. This behavior suggested that the xenon penetrated into this plane by a network of fine cracks. The cracks that are interconnected and give access to the xenon reservoir appear to be primarily oriented parallel to the bedding planes of this piece of coal and many are associated with the mineral-rich regions of the coal. In these cracks, the xenon pressure rapidly reached the reservoir pressure, but because the cracks are very fine on the scale of the CT resolution, the actual amount of xenon introduced into a voxel even when the crack had reached reservoir pressure was still quite small and so the CT signal in the difference image was small. As the xenon diffused into the coal away from the crack more xenon was introduced into the voxel containing the crack, and into neighboring voxels and consequently, the numbers on the difference image increased.

Figure 7 shows a composite plot of the CT numbers along the line drawn on the difference images of Figure 6. For the data along each line, the curve has been normalized to its maximum value. The plot illustrates the spreading of the xenon into the neighboring coal from a source apparently situated ca 2.5 mm from the arbitrary origin. It may be possible to analyze these curves in terms of a diffusion parameter which depends upon the CT number of the original coal.

A calibration graph of CT number against xenon pressure is given in Figure 8. This shows that if the xenon pressure at the high pressure inlet was 1130 torr, then the maximum observable CT number increase within an image of the coal should be 263, provided that all the xenon remained in the gas phase within the coal. In fact, CT numbers much greater than the gas phase maximum are observed within the CT difference image (Figure 6). This is probably caused by the xenon being present within the coal both as a gas phase species and as adsorbed species.

In the final image used in Figure 6, the maximum CT value along the line had risen to 2171, or over eight times the maximum possible from solely gas phase absorption. On the assumptions that the occupied surface area for a xenon atom is 22 (\AA)^2 (3) and a coal material density of 1.3 g/cm^3 , then the apparent surface area in a region with a xenon difference CT number of 2171 is $51 \text{ m}^2/\text{g}$. Using a BET apparatus, a room temperature xenon absorption measurement on a micronized sample of coal from the same batch gave a surface area of $44 \text{ m}^2/\text{g}$. The final image of xenon penetration into the coal could therefore be regarded as a surface area image for the coal. This information should be useful in future studies on the reactivity of coal.

The primary interest in the CT technique is in making use of its non-invasive nature for in situ studies of coal combustion and gasification. The preliminary studies discussed here will provide a basis for understanding the images obtained from more complex experiments.

ACKNOWLEDGMENTS

We would like to express our appreciation to the U.S. Department of Energy for support of this work (Contract No. DE-AC21-82MC19210).

REFERENCES

1. Maylotte, D.H., Lamby, E.J., Kosky, P.G., St. Peters, R.L., "Proceedings fo the International Conference on Coal Science", Dusseldorf, 1981.
2. Stach, E., Mackowsky, M.-th., Teichmuller, M., Teichmuller, R., Taylor, G.H., Chandra, D., (Eds.), Coal Petrology, Gerbruder Borntraeger, Berlin, 1975.
3. McClellan, A.L., Harnsberger, H.L., "Cross-Sectional Areas of Molecules Adsorbed in Solid Surfaces", Coll and Interface Sci., 23, 577 (1967).

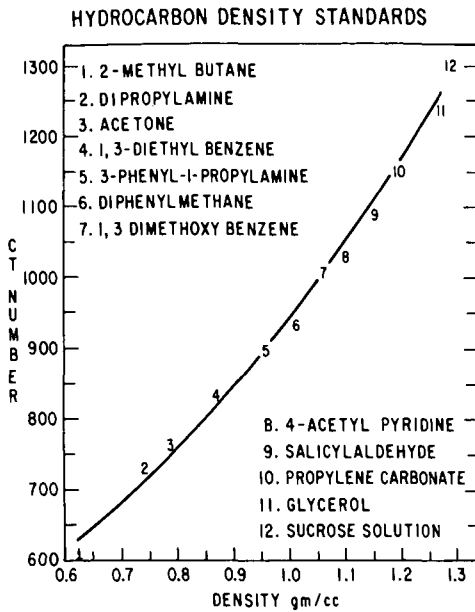


Figure 2. CT Number as a Function of Hydrocarbon Density

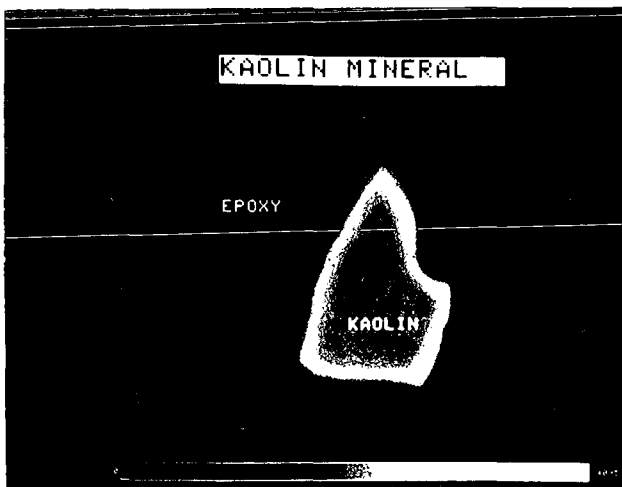


Figure 3. CT Image of Kaolin Sample Impregnated With Epoxy Around the Periphery

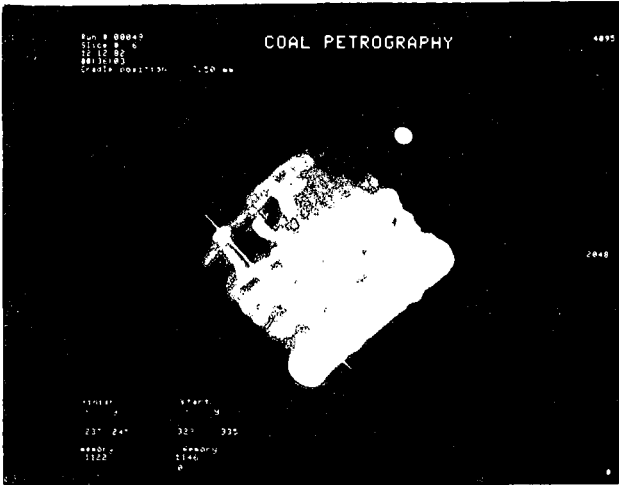


Figure 4a. CT Image of Illinois #6 Coal With a Line Drawn on the Image

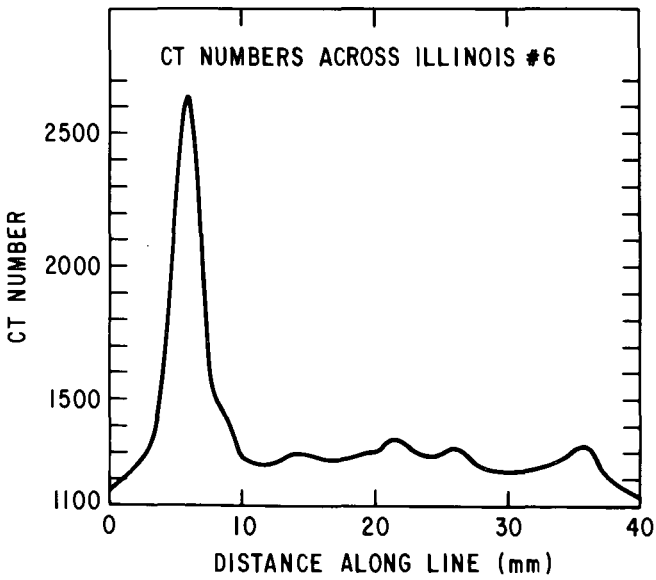


Figure 4b. CT Numbers Along the Line Drawn in Figure 4a

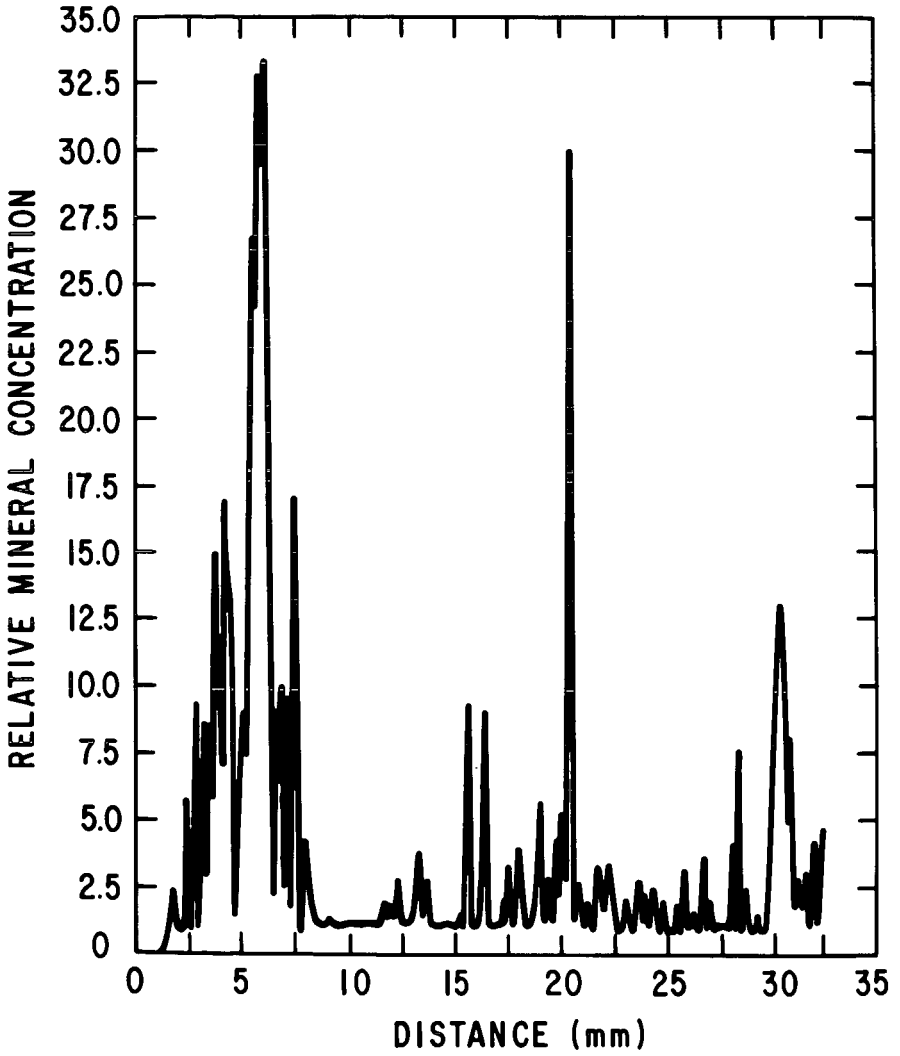


Figure 5. Relative Mineral Concentration Along the Line of Figure 4a.

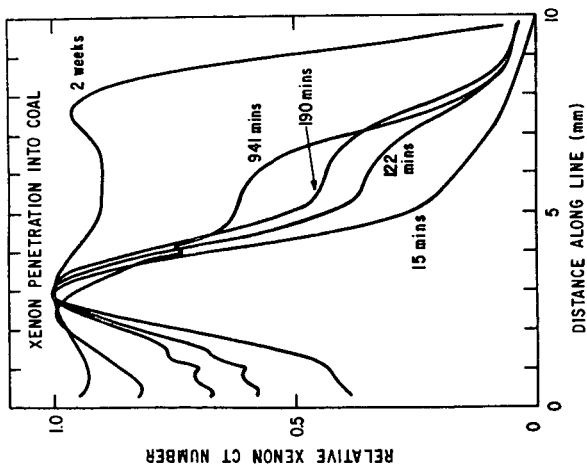


FIGURE 7. XENON PENETRATION INTO COAL ALONG THE LINE DRAWN IN FIGURE 6

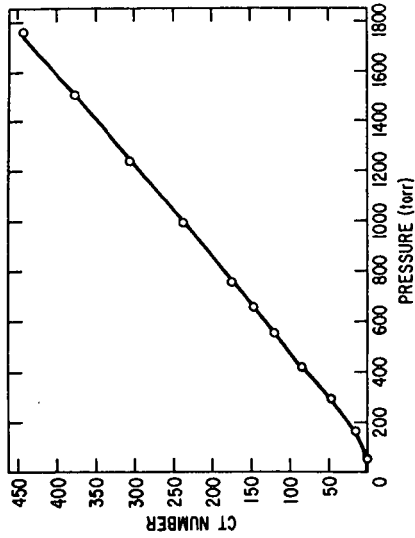


FIGURE 8. CT NUMBER AS A FUNCTION OF XENON GAS PRESSURE